Pharm Res (2010) 27:2544–2555
DOI 10.1007/s11095-010-0263-y

RESEARCH PAPER

Hyaluronic Acid/Chitosan-g-Poly(ethylene glycol) Nanoparticles for Gene Therapy: An Application for pDNA and siRNA Delivery

Manuela Raviña • Eva Cubillo • David Olmeda • Ramón Novoa-Carballal • Eduardo Fernandez-Megia • Ricardo Riguera • Alejandro Sánchez • Amparo Cano • María José Alonso

Received: 25 February 2010 / Accepted: 30 August 2010 / Published online: 21 September 2010

ABSTRACT

Purpose To design hyaluronic acid (HA) and chitosan-g-poly (ethylene glycol) (CS-g-PEG) nanoparticles intended for a broad range of gene delivery applications.

Methods Nanoparticles formulated at different HA/CS-g-PEG mass ratios were developed to associate either pDNA or siRNA. The physico-chemical characteristics, morphology, association efficiency and nuclease protection ability of the nanocarriers were compared for these two molecules. Their biological performance, including transfection effciency, nanoparticle cellular uptake and citotoxicity, was assesed.

Results The resulting nanoparticles showed an adequate size (between 130 and 180 nm), and their surface charge could be modulated according to the nanoparticle composition (from +30 mV to −20 mV). All prototypes exhibited a greater association efficiency and nuclease protection for pDNA than for siRNA. However, cell culture experiments evidenced that HA/CS-g-PEG nanoparticles were effective carriers for the delivery of both, siRNA and pDNA, eliciting a biological response with minimal cytotoxicity. Moreover, experiments performed in the HEK-EGFP-Snail1 cell line showed the potential of the HA/CS-g-PEG nanoparticles to silence the expression of the Snail1 transcription factor, an important mediator in tumor progression.

Conclusions HA/CS-g-PEG nanoparticles can be easily modulated for the delivery of different types of gene molecules, offering great potential for gene therapy applications, as evidenced by their biological performance.

KEY WORDS cancer therapy · chitosan · gene delivery · hyaluronic acid · nanoparticles

Electronic Supplementary Material The online version of this article (doi:10.1007/s11095-010-0263-y) contains supplementary material, which is available to authorized users.

M. Raviña • A. Sánchez • M. J. Alonso
Departamento de Farmacia y Tecnología Farmacéutica, Facultad de Farmacia
Universidad de Santiago de Compostela
Avda. de las Ciencias s/n
15782 Santiago de Compostela, Spain

E. Cubillo
Instituto Nacional de Toxicologia y Ciencias Forenses (INTCF)
Servicio de Biología
Las Rozas de Madrid
28032 Madrid, Spain

D. Olmeda
Centro Nacional de Investigaciones Oncologicas (CNIO)
Melchor Fernandez
Almagro, 4
28029 Madrid, Spain

R. Novoa-Carballal • E. Fernandez-Megia • R. Riguera
Department of Organic Chemistry and Center for Research in Biological Chemistry and Molecular Materials
University of Santiago de Compostela
Jenaro de la Fuente s/n
15782 Santiago de Compostela, Spain

A. Cano
Departamento de Bioquímica
Instituto de Investigaciones Biomédicas 'Alberto Sols' CSIC-UAM
c/Arturo Duperier
Madrid, Spain

M. J. Alonso (✉)
Department of Pharmacy and Pharmaceutical Technology
School of Pharmacy, University of Santiago de Compostela
15782 Santiago de Compostela, Spain
e-mail: mariaj.alonso@usc.es

INTRODUCTION

Nucleic acid-based therapeutics are envisioned to play a significant role in the next generation of treatments for a variety of diseases such as cancer. In the past, the common approach for gene therapy has been the delivery of DNA to replace a defective gene in the target-cell genome. Recently, the demonstration that RNA interference mediated by small-interfering RNA (siRNA) operated in mammalian cells (1) has opened up new possibilities to develop highly specific RNA-based gene silencing-therapeutics. Nevertheless, siRNA delivery suffers from many of the same limitations as DNA, such as poor cellular uptake and rapid degradation by ubiquitous nucleases. Therefore, as in the case of DNA therapy, the effective delivery is the most challenging hurdle remaining for the wide application of siRNA-based therapeutics (2).

Among the different gene delivery vehicles, polymer-based nanostructures have attracted increasing attention because of their versatility and, thus, their wide range of gene delivery applications. Among them, chitosan (CS)-based carriers (both polyplexes and nanoparticles) are an appealing approach due to their interesting properties and their efficiency in delivering genetic material, including plasmid DNA (pDNA) (3), oligonucleotides (4) and siRNA (5,6). Within this context, we have recently reported the feasibility and efficacy of nanoparticles made of poly(ethylene glycol)-grafted CS (PEG-g-CS) and also those from hyaluronic acid (HA) and CS as delivery carriers for pDNA (7–10). The results of this previous work indicated that the presence of either PEG or HA in the polymer nanostructure has a very positive role, not only in terms of enhancing their transfection capacity but also in terms of improving the toxicity profile of classical CS-based nanosystems.

In the rational design of novel siRNA or pDNA delivery systems, several considerations should be taken into account. siRNA and pDNA share common properties, i.e. they are both double-stranded nucleic acids with anionic phosphodiester backbones and identical negative charge/nucleotide ratio. The major two differences between these molecules rely on (i) pDNA used in gene therapy is often several kilo base pairs long, whereas siRNA typically consist of 19- to 21- nucleotide double-stranded RNAs; (ii) DNA gene therapy requires delivery of a pDNA into the host cell nucleus where it can induce expression of the desired gene, whereas siRNA has to travel simply to the cytosol to reach its target mRNA. Consequently, pDNA and siRNA gene therapy differ not only in their action mechanisms, but also in the cellular compartment where each mechanism is carried out. For these reasons, the experience in years with pDNA delivery has provided a good starting point for designing siRNA delivery systems (11,12). However, for a more rational design, technologies should be adapted to suit each molecule individually. It is currently accepted that elucidating these differences will help in the rational development of future delivery systems for specific gene delivery applications.

The aim of this work was to design a delivery system with a low toxicity profile that could be applied for a broad range of gene delivery applications, such as pDNA or siRNA delivery. For this purpose, we chose specific biomaterials which have shown beneficial properties not only from the biocompatibility point of view, but also from the perspective of their efficacy for pDNA delivery. Thus, we developed and characterized nanoparticles consisting of HA and CS-g-PEG. Moreover, in order to provide some insights into the rational development of gene delivery carriers, special emphasis has been placed on elucidating the impact that different molecules, pDNA *vs.* siRNA, have on the nanoparticle formulation. Thus, the physico-chemical characteristics, morphology, association efficiency and nuclease protection ability of the nanocarrier were compared for these two molecules. The resulting nanosystems were also evaluated with regard to their biocompatibility, cell internalization and capacity for gene transfer and gene knockdown. Finally, the ability of HA/CS-g-PEG nanoparticles to efficiently silence a recently described mediator of tumor invasion, the Snail1 transcription factor (13,14), was investigated.

MATERIALS AND METHODS

Materials

Sodium hyaluronate ophthalmic grade (having a molecular weight of around 170 kDa) was a gift from Bioiberica (Spain). Ultrapure chitosan hydrochloride salt (Protasan UP CL 110, CS·HCl), M_n 3.5×10^4, M_w 5.7×10^4 (determined by SEC-MALLS) (15) with 7% degree of acetylation (determined by ^{1}H NMR) (10) was purchased from FMC Biopolymers (Norway). Poly(ethylene glycol) monomethyl ether (MeO-PEG-OH, M_n 5055, M_w 5088, determined by MALDI-TOF) was purchased from Sigma-Aldrich. N-hydroxysuccinimide (NHS) and N-(3-dimethylaminopropyl)-N-ethylcarbodiimide hydrochloride (EDC·HCl) were purchased from Fluka (Spain). Plasmid DNA (pDNA)-encoding green fluorescent protein (pEGFP-C1) driven by a CMV promoter was purchased from Elim Biopharmaceuticals (San Francisco, CA, USA). EGFP-specific siRNA duplex containing the sequences sense: 5′-GCAAGCUGACCCUGAA GUUCTT-3′ antisense: 5′-GAACUUCAGGGUCAG CUUGCTT-3′ and Snail1-specific siRNA duplex containing the sequences sense 5′- CAAACCCACUCGGAUGUGA

AGAGAUTT-3′ antisense 5′-AUCUCUUCACAUCCGA GUGGGUUUGTT3′ were purchased from Invitrogen. siRNA non-specific sequences containing sense: 5′-UGCG CUAGGCCUCGGUUGCTT3′ and antisense 5′ GCAACCGAGGCCUAGCGCATT-3′ and EGFP siRNA containing a fluorescent Cy3 labeled sense strand used for cellular uptake studies were purchased from MWG (Germany). Chitosanase with an activity of 0.25 Umg^{-1} was purchased from Seikagaku Corp. (Japan). Mouse serum, pentasodium tripolyphosphate (TPP), Trizma® base, agarose, xylene cyanole, bromophenol blue, ethidium bromide (purity 95%), fluorescein-5-isothiocyanate, and MTT ((3-4,5-dimethylthiazol-2-yl)-2,5-diphenyltetrazolium bromide) were all purchased from Sigma Aldrich (Madrid, Spain). One kBp DNA ladder was obtained from Life Technologies (Barcelona, Spain). The PicoGreen® reagent was purchased from Molecular Probes (OR, USA). All other solvents and chemicals were of the highest grade commercially available.

Synthesis of PEG-g-CS

Grafting of PEG to chitosan was carried out by a carbodiimide-mediated reaction, using a carboxylic acid derivative of PEG (MeO-PEG-OCH_2CO_2H) as previously reported (10,16,17). MeO-PEG-OCH_2CO_2H was synthesized from a commercially available MeO-PEG-OH. CS·HCl (100 mg, 0.50 mmol) was dissolved in H_2O (14.3 ml). MeO-PEG-OCH_2CO_2H (17.8 mg, 3.40 mmol, M_n 5114) and NHS (2.02 mg, 0.017 mmol) were then added to the solution. Finally, EDC·HCl (26.9 mg, 0.140 mmol) was added in portions. The resulting solution was stirred at room temperature for 22 h and was then ultrafiltered (Amicon, YM30) and lyophilized to yield CS-g-PEG as white foam (105 mg). The degree of PEGylation was determined as 0.5% (equivalent to 11% in weight) according to ^1H NMR (2% DCl in D_2O).

Nanoparticle Preparation

Nanoparticles were prepared by the ionotropic gelation technique according to the methodology previously developed by our group (7,18). The hyaluronic acid solution (HA), mixed with the cross-linker TPP, was added over the (CS-g-PEG) solution under magnetic stirring. Agitation was maintained for 10 min to allow the complete formation of the system. The CS-g-PEG solution was prepared at a concentration 0.625 mg/mL in ultrapure water (0.75 mL). The TPP concentration was kept constant (0.5 mg/mL), and a fixed volume (50 μL) was mixed with the HA solution prior to the formation of the nanoparticles. To modulate the weight ratio of the polysaccharides that constitute the nanoparticles (HA/CS-g-PEG 1/2, 1/1, or 2/1), we varied the concentration and volumes of the HA solution (0.625 or 1.25 mg/mL and 0.375 or 0.750 mL, respectively). For the association of the pDNA or siRNA, these were added to the HA/TPP solution in small volumes that varied depending on the theoretical loading. These were fixed at 1%, 2.5%, 5% or 10% with respect to the total amount of the polysaccharides (HA and CS-g-PEG) used for the formulation of the nanoparticles (mg of pDNA or siRNA/100 mg of polysaccharides).

Eventually, nanoparticles were concentrated by centrifugation (Beckman Avanti TM 30, Beckman, Spain) on a glycerol bed.

Nanoparticles composed solely of CS-g-PEG were also prepared by ionic gelification. In this case, 0.4 mL of TPP at a concentration of 0.83 mg/mL were added over 1 mL of CS-g-PEG (1 mg/mL).

Nanoparticle Characterization

Size and Zeta Potential Measurements

The mean particle size and the size distribution of the nanoparticles were determined by photon correlation spectroscopy (PCS). Samples were diluted with filtered water. The zeta potential values of the nanoparticles were obtained by Laser Doppler Anemometry (LDA), measuring the mean electrophoretic mobility. Samples of the nanoparticle suspensions were diluted with 1 mM KCl. The PCS and LDA analysis were performed with a Zetasizer® 3000HS (Malvern Instruments, UK).

pDNA and siRNA Association Efficiency

The association of the pDNA or siRNA to the nanoparticles was determined by gel electrophoresis assays (1% or 2% agarose, respectively, containing ethidium bromide, 50 V, 120 min, Sub-Cell GT 96/192, Bio-Rad Laboratories Ltd., England).

The association efficiency was also calculated from the amount of non-associated siRNA, which was recovered in the supernatant samples collected upon the centrifugation of the nanoparticles (10.000 RFC, 40 min, Avanti 30 Beckman, Barcelona, Spain). The amount of free siRNA was determined by fluorimetry (LS 50B luminescence spectrometer, Perkin-Elmer) using the PicoGreen® reagent (Molecular Probes, OR, USA).

Morphology of the Nanoparticles

The morphology of the nanoparticles was examined by transmission electron microscopy at 100 kV (CM 12 Philips, Eindhoven, The Netherlands) using samples stained with a 2% phosphotungstic acid solution and placed on copper grids (400 mesh) coated with a Formvar® film.

Nuclease Protection Assay

DNase I Protection Assay

Ninety μL of naked or pDNA associated to the nanoparticles were incubated with 10 μL of DNase I (1 unit of DNase I per 1 μg of pDNA) in the presence of 5 mM magnesium chloride and 1 mM calcium chloride. The samples were incubated under horizontal shaking for 1 h at 37°C. The enzymatic reaction was terminated by the addition of 5 μL of 0.5 M EDTA. For pDNA recovery after DNase I treatment, samples were incubated with chitosanase during 4 h (0.7 U per mg of nanoparticle). The topology of the pDNA was eventually determined by a conventional 1% agarose gel electrophoresis assay.

Serum Stability

Naked siRNA and siRNA associated to the nanoparticles were incubated with mouse serum at a final 50% mouse serum concentration under horizontal shaking for 4 h at 37°C. Displacement of the nucleic acid from the particles was achieved by adding heparin to the sample immediately before loading the samples on a 2% agarose gel.

Cell Culture Studies

HEK293T human embryonic kidney cells were cultured in Dulbeco Modified Eagle Medium (DMEM) supplemented with 10% foetal bovine serum, 2 mmol/L of L-glutamine, and antibiotics at 37°C in a humidified 5% CO2 atmosphere

Generation of HEK-EGFP and HEK-EGFP-Snail1 Cell Lines

HEK293T stable transfectants were obtained by the transfection of 3 μg of either pEGFPC1 or pEGFP-C1-Snail1 vectors as described in (19) using Lipofectamine Reagent (Invitrogen) according to the manufacturer's instructions. EGFP-positive cell populations were selected by three rounds of bulk sorting on a FACSVantage cell sorter (Becton-Dickinson) and subsequently cloned by single cell deposition in 96-well plates containing 200 μL supplemented medium per well by the automated cell deposition unit of the FACSVantage cell sorter. After 2 to 3 weeks, three single colonies were analyzed by flow cytometry and western-blot analysis for the presence EGFP and EGFP-Snail1 expression (20).

Cell Toxicity Studies

The cytotoxicity of the nanocarriers was studied in the cell line HEK293T using the MTT colorimetric assay. MTT is a yellow tetrazolium salt that is reduced only in living, metabolically active cell mitochondria. Cells were seeded at a density of 6×10^4 cells per well into 96-multiwell culture plates (Costar, Cambridge, UK) 24 h before the experiment. Increasing doses of the pDNA-loaded nanoparticles (from 6.36 to 101.81 $\mu g/cm^2$) were incubated with the cells for 5 h. Afterwards, the nanoparticles were removed and replaced by the MTT solution (1 mg/mL). The plates were further incubated for 4 h at 37°C (protected from light). The medium was then removed, and the formazan crystals formed in each well were dissolved with 100 μL of DMSO. Absorbance values were measured at 570 nm using a microplate reader. Cell viability, as a percent of the non-treated cells, was calculated from the absorbance values.

pDNA Transfection Studies

HEK293T cells were seeded at a density of 3×10^5 cells per well into 24-multiwell culture plates (Costar, Cambridge, UK) and were allowed to grow for 24 h before transfection. Cells were washed and the culture medium replaced by 300 μL of Hanks' balanced salt solution (HBSS, pH 6.4). pDNA-loaded nanoparticles were added to the cells (1 μg pDNA/well). After 5 h, the medium was replaced with 1 mL of fresh cell culture medium. Four days post-transfection, GFP-positive cells were detected by fluorescence microscopy. Fluorescence images were obtained using a fluorescence microscope (Eclipse TE 2000-S, Nikon UK Ltd, UK) equipped with a digital camera (Nikon E4500).

Gene Knockdown Experiments

HEK-EGFP and HEK-EGFP-Snail1 cells were seeded at a density of 2×10^5 cells per well into 24-multiwell culture plates (Costar, Cambridge, UK) and were allowed to grow for 24 h before transfection. Cells were washed and the culture medium replaced by 300 μL of Hanks' balanced salt solution (HBSS, pH 6.4). HA/CS-g-PEG 1/1 5% siRNA-loaded nanoparticles were added to the cells (100 nM siRNA/well). After 3 h, the medium was replaced with 1 mL of fresh cell culture medium. Lipofectamine 2000-siRNA transfection (100 nM siRNA/well) was performed according to the manufacturer's instructions. Three days post-transfection, cells were trypsinized and resuspended in PBS with 2% (v/v) of FBS. The EGFP cell fluorescence was measured using a Becton-Dickinson FACSCalibur flow cytometer. A histogram plot with log green fluorescence intensity on the x-axis and cell number on the y-axis was used to define median fluorescence intensity of the main cell population defined by scatter properties (forward and side scatter).

Cellular Uptake Studies

HA/CS-g-PEG 1/1 nanoparticles were loaded with 2.5% Cy3-labelled siRNA according to the procedure described before. HEK-EGFP-Snail1 cells were seeded at a density of 2×10^5 cells per well, on sterile glass covers previously coated with poly-L-lysine (Sigma-Aldrich, Spain) and placed in 24-multiwell culture plates (Costar, Cambridge, UK). Twenty-four h later, the loaded nanoparticles were incubated with the cells (50 nM siRNA/well). After 3 h incubation, cells were rinsed with PBS and fixed with 4% paraformaldehyde. Afterwards, they were permeabilised with 0.1% Triton-X100, the cell nuclei were stained with DAPI, and F-actin was stained with BODIPY-phalloidin according to the manufacturer's instructions. Finally, the cell fluorescence was analysed with a confocal laser scanning microscope (Leica TCS SP2, Leica Microsystems). Laser excitation wavelengths of 405 nm, 488 nm, 561 nm and 633 nm were used, and fluorescent emissions from DAPI (emission $\lambda=415$–470 nm), EGFP (emission $\lambda=495$–540), Cy3 (emission $\lambda=580$–625) and Bodipy-phallodin (emission $\lambda=645$–710 nm) were collected using a sequencial scan.

Statistical Analysis

The statistical significance was studied by the one-way ANOVA followed by a multiple comparison analysis (SigmaStat Program, Jandel Scientific, version 2.0). Differences were considered to be significant at a level of $p<0.05$.

RESULTS AND DISCUSSION

As indicated in the introduction, the overall goal of this work was to develop a new nanoparticle formulation, composed of HA and CS-g-PEG that could be applied for a broad range of gene delivery applications, such as pDNA or siRNA delivery. The rationale behind the combination of these biomaterials was based on the previously observed positive role of HA and PEG incorporated separately into CS nanoparticles. In fact, as indicated in the introduction, HA/CS and CS-g-PEG nanoparticles have exhibited clear benefits in terms of pDNA delivery compared to classical CS nanoparticles (8–10,21).

Moreover, a special emphasis has been made on the understanding of the differences determined by the association of pDNA *vs.* siRNA on the resulting nanoparticle formulations and their behavior in biological media. We believe that elucidating these differences will facilitate the rational development of future delivery systems for specific gene delivery applications.

Preparation of pDNA and siRNA-Loaded HA/CS-g-PEG Nanoparticles

Previous works from our laboratory have shown that ionic gelation is a suitable technique for the preparation of pDNA-loaded CS-g-PEG (10) and pDNA-loaded HA/CS nanoparticles (21). On the other hand, with regard to siRNA, it has been reported that its entrapment into CS nanoparticles leads to a significant biological effect (6). This effect was significantly higher than that observed after simple complexation or adsorption onto preformed CS nanoparticles, a fact that was attributed to the better protection against nuclease degradation of the entrapped molecule (6). For these reasons, the ionic gelation technique has been adapted in order to develop HA/CS-g-PEG nanoparticles in the presence of the ionic crosslinker tripolyphosphate (TPP). The mechanism of formation combines the electrostatic interaction between both polysaccharides (HA and CS-g-PEG), which are oppositely charged, with the known cross-linking ability of TPP (18).

For the development of HA/CS-g-PEG nanoparticles, the amount of CS-g-PEG and crosslinker were fixed, while the amount of HA was modified in order to obtain nanoparticles with different HA/CS-g-PEG mass ratios (1/2, 1/1 and 2/1). Table 1 shows the effect of nanoparticle composition on the particle size, polydispersity index, and zeta potential for the HA/CS-g-PEG mass ratios studied. The nanoparticles were found to have a narrow size distribution, irrespective of their composition. In agreement with previous observations (9), the influence of the negatively charged HA on the nanoparticle surface charge was evidenced, as zeta potential values were inverted with the increase of HA content in the formulation.

For the entrapment of pDNA into the nanoparticles, a theoretical pDNA loading of 10% was fixed (wt/wt, based on the weight of HA and CS-g-PEG). As depicted in Table 1, this great pDNA loading causes some changes in the inherent characteristics of the nanoparticles. First, the size of the pDNA-loaded nanoparticles slightly increased compared to that of the blank formulation. Second, as expected, the positive zeta potential values of the 1/1 HA/CS-g-PEG formulation were inverted due to the negatively charged phosphate groups in the pDNA backbone.

For the development of siRNA-loaded nanoparticles, we also started with a theoretical siRNA loading of 10% wt/wt. However, this great loading led to the precipitation of the formulations, highlighting the necessity of an adequate formulation of the nanosystem for each individual molecule. This fact was probably due to an excess of negative charges available in the siRNA molecules in relation to the amino-positive groups in the cationic polysaccharide. This distinct behavior of siRNA, when compared to pDNA, could be explained by some structural differences of both molecules

Table I Physico-chemical Characterization of Hyaluronic Acid and Poly(ethylene glycol)-Grafted Chitosan (HA/CS-g-PEG) Nanoparticles Formulated at Different Mass Ratios (wt/wt) (means±s.d., $n=3$)

HA/CS-g-PEG mass ratio	Blank nanoparticles			pDNA-loaded nanoparticles[a]			siRNA-loaded nanoparticles[b]		
	Size (nm)	PI	ζ (mV)	Size (nm)	PI	ζ (mV)	Size (nm)	PI	ζ (mV)
1:2	–[c]	–	–	166.1±0.9	0.28–0.31	+31.9±2.7	–[c]	–	–
1:1	130.9±8.5	0.17–0.22	+15.2±2.5	154.5±2.9	0.07–0.14	−0.9±0.2	150.8±10.5	0.11–0.13	+8.9±3.9
2:1	158.5±1.3	0.17–0.19	−17.6±5.2	176.6±11.6	0.25–0.36	−20.1±4.1	250.6±22.4	0.22–0.48	−18.1±1.19

CS-g-PEG dissolved in water at 0.625 mg/ml. HA dissolved in water at 0.625 mg/ml or 1.25 mg/ml. CS-g-PEG/TPP mass ratio 18.75/1. PI: polydispersity index

[a] The theoretical pDNA loading was fixed at 10% (wt/wt).

[b] The theoretical siRNA loading was fixed at 5% (wt/wt).

[c] Nanoparticles not formed.

and their condensation process. In fact, pDNA is easily condensed when around 90% of its phosphodiester backbone charge is neutralized (22). In contrast, condensation of siRNA molecules (with a 21 base pairs length) cannot occur during the nanoparticle formation process (a minimal length of nucleic acid of about 400 base pairs is required for condensation (23)), thus resulting in an excess of negative charges and the subsequent precipitation of the system. For that reason, we decided to reduce the theoretical siRNA loading to 5% wt/wt. Using this loading, it was possible to obtain nanoparticles with a HA/CS-g-PEG 1/1 and 2/1 mass ratios. Given the more appropriate size range, the HA/CS-g-PEG 1/1 formulation was selected for further experiments.

In a second step, the effective association of pDNA or siRNA to the nanoparticles was assessed using a gel retardation assay. For pDNA-loaded formulations, no migration of free pDNA was observed in any case, indicating that all pDNA was effectively associated to the nanoparticles (Fig. 1a). However, the situation was slightly different in the formulations containing siRNA. Indeed, in Fig. 1b it can be noted that for the higher siRNA loadings (2.5% and 5%), a small amount of siRNA is present in the free form. According to the Picogreen® assay, the siRNA association efficiency was 78.7±1.8 and 79.1±5.7%, respectively. Consequently, both pDNA and siRNA can be efficiently entrapped within these nanoparticles with optimal association values (100%) for pDNA. The greater association of pDNA, when compared to siRNA, has also been observed for PEG-PEI/siRNA complexes (24) and chitosan/siRNA complexes (6). This could be due to the different interaction of a pDNA or a siRNA with the nanoparticle formulation. In fact, although the complexation of both nucleic acids with polycations relies on electrostatic interactions, short polynucleotides are considered to be particularly difficult in this respect due to their limited number of negative charges per molecule not being sufficient for cooperative binding (25) and behaving as rigid rods (26). As a consequence, their disordered interactions within the nanoparticles may result in incomplete association.

Nanoparticle Morphology

The size and morphology of the nanoparticles containing pDNA or siRNA were observed by transmission electron microscopy. As can be seen in Fig. 2, irrespective of the associated molecule, homogenous populations of spherical-

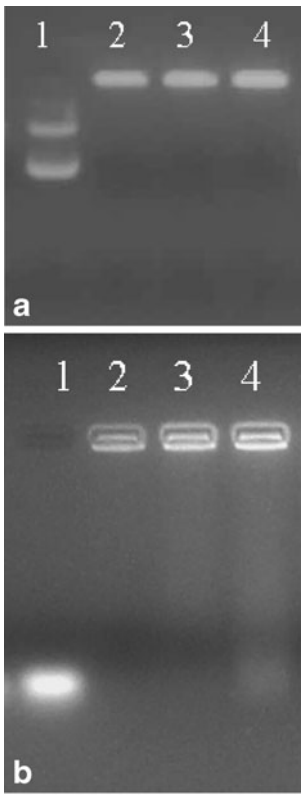

Fig. 1 **a** Gel retardation assay for 10% pDNA-loaded HA/CS-g-PEG nanoparticles formulated at different mass ratios: 1/2 (lane 2), 1/1 (lane 3) and 2/1 (lane 4). Lane 1: naked pDNA. **b** Gel retardation assay for siRNA-loaded HA/CS-g-PEG 1/1 nanoparticles formulated at 1% (lane 2), 2.5% (lane 3) and 5% (lane 4) theoretical siRNA loadings. Lane 1: naked siRNA.

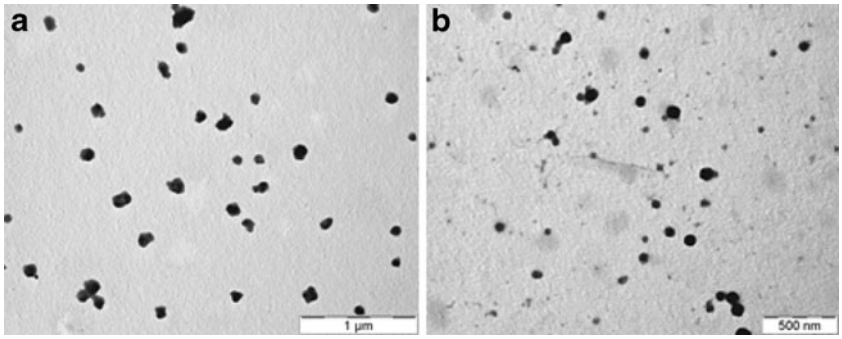

Fig. 2 Morphology of HA/CS-g-PEG-loaded nanoparticles as visualized in transmission electron microscopy (TEM): 1/1 HA/CS-g-PEG 10% pDNA-loaded nanoparticles (**a**); 1/1 HA/CS-g-PEG 5% siRNA-loaded nanoparticles (**b**).

shaped nanoparticles with average size lower than 200 nm were obtained. Moreover, this morphology is similar to that previously observed for nanoparticles made of solely CS (18) or CS in combination with other biopolymers such as HA (7).

Nuclease Protection Assay

For efficient *in vivo* delivery, it is essential that a synthetic vector can protect the genetic material from degradation during its transport to the target cells. Thus, adequate protection of pDNA and siRNA is crucial in gene therapy applications. The DNase I protection assay is a general procedure to evaluate the nuclease protection of pDNA. In order to verify whether HA/CS-g-PEG nanoparticles were able to efficiently protect pDNA from nuclease degradation, they were incubated for 1 h with DNase I. Then, nanoparticles were incubated with chitosanase (an enzyme that degrades chitosan) for pDNA recovery. Subsequently, the released pDNA was loaded in an electrophoresis gel to asses its integrity. Nanoparticle protection from DNase I degradation is shown in Fig. 3. Naked pDNA treated with DNase I was completely degraded (lane 3), whereas pDNA recovered from the nanopaticles was protected (lanes 9, 10, 11). A reduction of the fraction of supercoiled pDNA released from the nanoparticles was observed for the HA/CS-g-PEG 1/1 and 2/1 nanoparticles (lanes 10 and 11). However, this reduction was comparable to that observed when naked pDNA (lane 4) was incubated with chitosanase (lane 5). This was probably due to the activity of additional enzymes present in commercially available chitosanase extracts. Accordingly, it can be concluded that HA/CS-g-PEG nanoparticles efficiently protect pDNA from nuclease degradation.

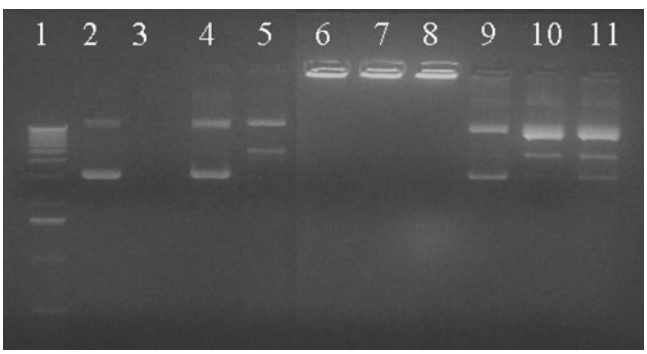

Fig. 3 Nuclease stability of pDNA associated to HA/CS-g-PEG nanoparticles. *Lane 1*: DNA ladder; *lane 2*: naked pDNA; *lane 3*: naked pDNA+ DNase I; *lane 4*: naked pDNA; *lane 5*: naked pDNA+ chitosanase; *lane 6*: HA/CS-g-PEG 1/2 pDNA NP + DNase I; *lane 7*: HA/CS-g-PEG 1/1 pDNA NP + DNase I; *lane 8*: HA/CS-g-PEG 2/1 pDNA NP + DNase I; *lane 9*: HA/CS-g-PEG 1/2 pDNA NP + DNase I+ chitosanase; *lane 10*: HA/CS-g-PEG 1/1 pDNA NP + DNase I+ chitosanase; *lane 11*: HA/CS-g-PEG 2/1 pDNA NP + DNase I+ chitosanase.

In the case of siRNA, the general procedure for the evaluation of nuclease protection is the treatment with serum, a nuclease-rich medium (27). Thus, siRNA-loaded HA/CS-g-PEG nanoparticles were incubated in a final 50% mouse serum concentration at 37°C for up to 4 h and then treated with heparin in order to displace the associated siRNA (6). Finally, the integrity of the siRNA molecules was assessed in an electrophoresis gel. Figure 4 shows that naked siRNA totally degrades in serum (lane 3), whereas the one associated to the nanoparticles is significantly protected from degradation (lane 4).

Overall, the comparison of the stability results of pDNA and siRNA led us to conclude the protective role of the nanoparticles. However, the degree of protection is visually higher in the case of pDNA. This could be explained by the

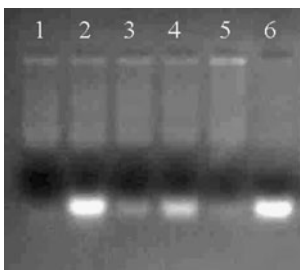

Fig. 4 Nuclease stability of siRNA associated to 5% loaded HA/CS-g-PEG 1/1 nanoparticles. *Lane 1*: serum + heparin; *Lane 2*: naked siRNA + heparin; *Lane 3*: naked siRNA + serum + heparin; *Lane 4*: HA/CS-g-PEG siRNA NP + serum + heparin; *Lane 5*: HA/CS-g-PEG siRNA NP + serum; *Lane 6*: HA/CS-g-PEG siRNA NP + heparin.

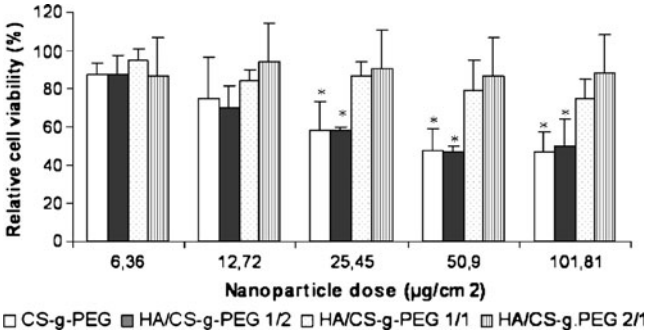

Fig. 5 Cell viability upon exposure to increasing doses of 10% pDNA loaded nanoparticles. Different nanoparticle formulations are represented as CS-g-PEG (*white bars*), HA/CS-g-PEG 1/2 (*grey bars*), HA/CS-g-PEG 1/1 (*dotted bars*) and HA/CS-g-PEG 2/1 (*stripped bars*). Results are expressed as mean ± S.D. ($n = 3$). Statistical differences are denoted as * ($p < 0.05$).

greater susceptibility of siRNA to degrade compared to DNA, as well as by its inability to condense in the presence of cationic polymers. On one hand, siRNA molecules contain ribose, a sugar with a hydroxyl group in the 2′ position, which makes the RNA backbone highly susceptible to hydrolysis by serum nucleases (28). On the other hand, the condensation of pDNA molecules with cationic polycations provides an important protection of the DNA chains from the external medium (29), whereas this condensation is not feasible for siRNA molecules.

Cell Toxicity Studies

An important challenge for the success of gene-based therapies is the development of acceptable and efficient delivery systems with minimal toxicity and maximum patient safety. There is previous information on the cellular toxicity of chitosan-based nanocarriers (30). In this context, it is known that the incorporation of PEG groups on CS nanoparticles has a positive role in reducing CS nanoparticle toxicity (10). Also, the incorporation of HA into CS nanoparticles has been shown to reduce their toxicity profile (9). For these reasons, in this work we decided to take advantage of the beneficial effects of both PEG and HA and developed a new gene carrier with a very low toxicity profile. The effect of HA/CS-g-PEG nanoparticles on cell viability was studied by determining their effect in the metabolic activity of HEK293T cells, following incubation for up to 5 h. HA/CS-g-PEG nanoparticles formulated at different mass ratios and associating pDNA were evaluated. Previously developed CS-g-PEG nanoparticles were used as a control (10). The percentage of cell viability as a function of the nanoparticle dose ($\mu g/cm^2$) is depicted in Fig. 5. The toxicity of the nanoparticles remains acceptable for up to 12.72 $\mu g/cm^2$, a concentration which surpasses the one required for efficient cell transfection. However, differences between formulations were observed

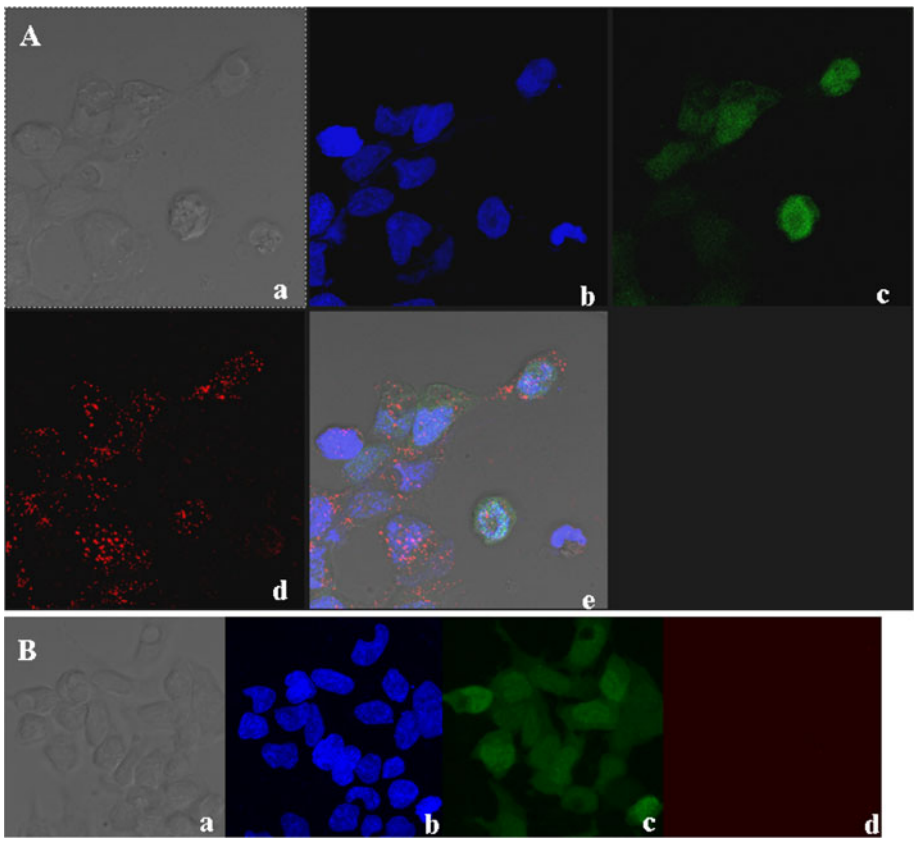

Fig. 6 Confocal fluorescence microscopy images in HEK-EGFP-Snail1 cells. The cell line is stably expressing the fusion EGFP-Snail1 protein and the cell nuclei were stained with DAPI. Full-sized images of each of the three separate channels and the overlaid image are shown. Maximum projections after siRNA-Cy3 loaded HA/CS-g-PEG 1/1 nanoparticles incubation, panel A (a,b,c,d,e) and after naked siRNA-Cy3 incubation, panel B (a,b,c,d) corresponding to (**a**) phase contrast image, (**b**) nuclear DAPI staining, (**c**) EGFP-Snail1 (green), (**d**) Cy3 (red), (**e**) merge image. Images were acquired at a magnification of 63×.

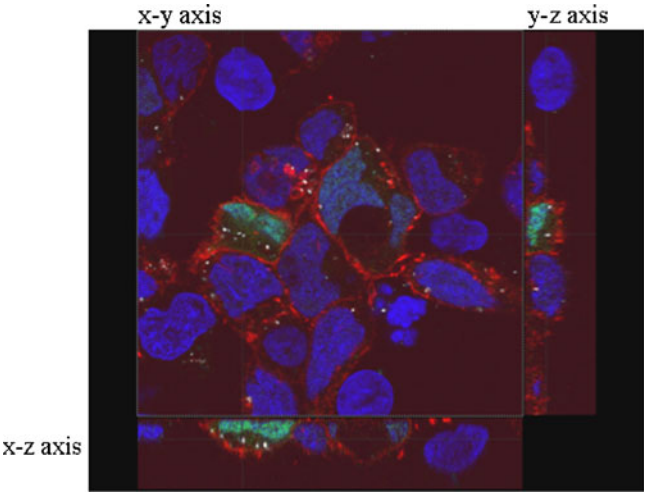

Fig. 7 Confocal fluorescence microscopy image in HEK-EGFP-Snail1 cells. Detailed image of a cross-section in the x-y, y-z and x-z axis after siRNA-Cy3-loaded HA/CS-g-PEG 1/1 nanoparticles incubation (*white*). The cell line is continuously expressing the fusion EGFP-Snail1 protein (*green*), the cell nuclei were stained with DAPI (*blue*) and the F-actin filaments of the cytoskeleton were stained with phalloidin (*red*). Images were acquired at a magnification of 63×.

for higher nanoparticle concentrations. As shown in Fig. 5, formulations containing higher amounts of HA (HA/CS-g-PEG 1/1 and 2/1) showed a decreased toxicity profile compared to the CS-g-PEG or HA/CS-g-PEG 1/2 formulations ($p<0.05$). This can be supported by the high biocompatibility of the glycosaminoglycan hyaluronan. In fact, HA is a major constituent of the extracellular matrix, essential for proper cell growth, organ structural stability and tissue organization (31). Therefore, the low toxicity profile of HA/CS-g-PEG nanoparticles renders this nanosystem a safe gene delivery vehicle.

Nanoparticle Cellular Uptake Studies

We recently reported the potential of HA/CS nanoparticles for the intracellular delivery of pDNA (9,21). In this case, our goal was to evaluate if the newly developed HA/CS-g-PEG nanoparticles retain this capacity to enter cells. For that purpose, Cy3-labelled siRNA (Cy3-siRNA) was associated to nanoparticles and their uptake evaluated by the HEK-EGFP-Snail1 cells stably expressing the fusion EGFP-Snail1 protein (green). The cell nuclei were stained with DAPI (blue). The confocal images of HEK-EGFP-Snail1 cells (Fig. 6) show an intense red signal corresponding to the effective internalization of the siRNA (Fig. 6a). Meanwhile, no red signal was detected after incubation of the cells with naked Cy3-siRNA (Fig. 6b). Furthermore, in order to specifically localize the siRNA intracellularly, the F-actin filaments of the cells (cytoskeleton) were also stained with phalloidin. In this case, phalloidin is shown in red and siRNA-Cy3 in white. The images of the x-y, x-z and y-z cross-sections clearly illustrate the intracellular localization of the si-RNA-loaded nanoparticles (Fig. 7). This indicates that the nanoparticles are able to efficiently deliver siRNA intracellularly, thus providing a good indication of their potential as gene carriers.

Transfection Efficiency and Gene Knockdown Capacity

In addition to the cellular uptake of the nanoparticles, a prerequisite for the adequate transfection/silencing is the efficient delivery of the nucleic acid in its active form. In order to evaluate this capacity, HA/CS-g-PEG nanoparticles loaded with pDNA encoding the green fluorescent protein (pEGFP) were evaluated in the HEK293T cell line. As can be seen in Fig. 8a, b, c, effective gene transfection was observed for the different formulations of nanoparticles.

The evaluation of the gene silencing performance of the nanoparticles was studied in a model of endogenous gene knockdown, i.e. HEK-293 cells stably expressing the EGFP protein. For that purpose, siRNA against the EGFP protein (si-EGFP) was associated to the nanoparticles. The decrease in EGFP mean fluorescence intensity, detected by flow cytometry, was used as a measure of EGFP knockdown. As can be observed in Fig. 9, HA/CS-g-PEG nanoparticles

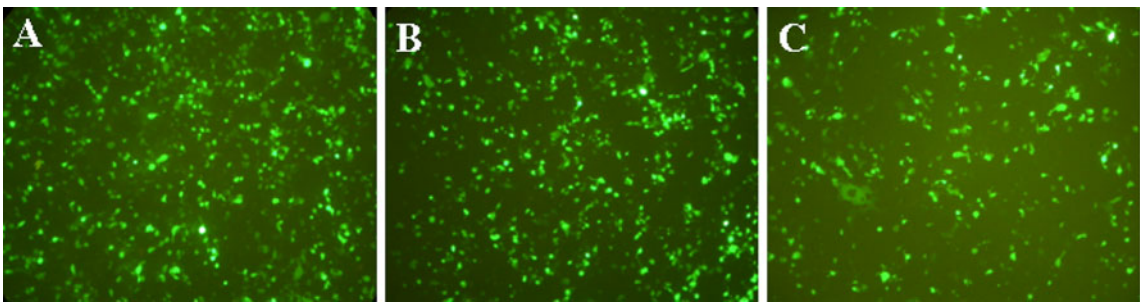

Fig. 8 Fluorescence micrographs of HEK293T cells transfected with 10% pDNA-loaded HA/CS-g-PEG nanoparticles (different mass ratios) (1 μg pDNA/well): HA/CS-g-PEG 1/2 nanoparticles (**A**); HA/CS-g-PEG 1/1 nanoparticles (**B**); HA/CS-g-PEG 2/1 nanoparticles (**C**). Images were acquired at 4 days post-transfection.

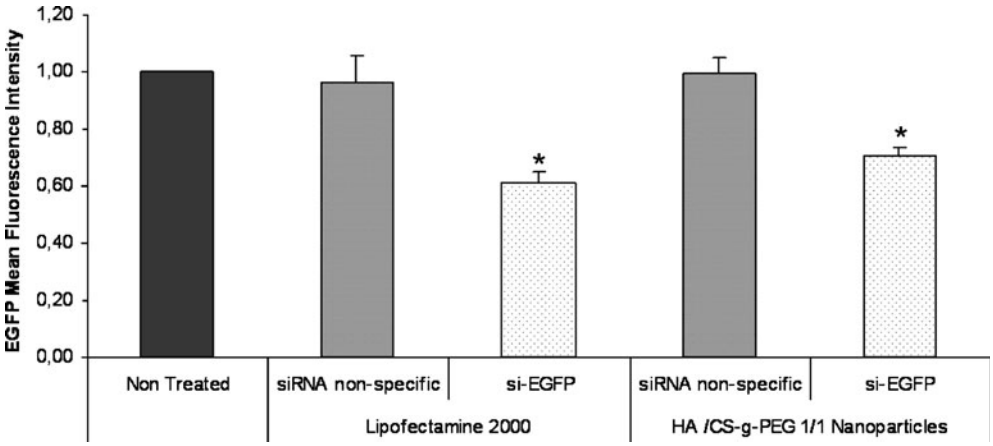

Fig. 9 Nanoparticle-mediated RNA interference in the HEK-EGFP cells. HA/CS-g-PEG 1/1 nanoparticles or Lipofectamine 2000 associating si-EGFP were incubated with the cells (100 nM siRNA/well). HA/CS-g-PEG 1/1 nanoparticles or Lipofectamine 2000 associating siRNA-non specific targeting negative controls are also shown. Results are expressed as mean±S.D. ($n=3$). Statistical differences are denoted as * ($p<0.05$).

associating siEGFP significantly silenced the EGFP expression, compared to non-treated cells. In contrast, HA/CS-g-PEG nanoparticles incorporating a non-specific siRNA did not show any knockdown effect. Moreover, the silencing effect observed for the siRNA-loaded nanoparticles was comparable to that of Lipofectamine 2000, a highly efficient commercially available transfection reagent. These results are in agreement with those previously reported for other CS-based delivery systems, where gene silencing levels had comparable effects to positive commercial controls (5,6,32). In addition, from a toxicological point of view, the incorporation of HA into the formulation has resulted in an improvement of the toxicological profile of the resulting CS-g-PEG-based nanosystems. Moreover, although this possibility has not been explored in this work, the incorporation of HA to the nanoparticle formulation represents an added value in terms of offering the possibility to achieve a selective targeting. In fact, in many cancers of epithelial origin there is an upregulation of CD44, a receptor that binds HA. For that reason, HA has been used as a drug carrier and a ligand on liposomes or nanoparticles to target drugs to CD44-overexpressing cells (33).

Taking into account the promising results obtained with the HA/CS-g-PEG nanoparticles for siRNA delivery and the excellent opportunities of siRNA in cancer treatment, we decided to evaluate the potential of this new nanocarrier to efficiently deliver a therapeutic siRNA. For this purpose, we chose a siRNA targeting the Snail1 transcription factor, a factor that was recently proposed as an important mediator of tumor invasion (13,14). The rationale behind this selection from a therapeutical standpoint is that metastasis is of great importance to the clinical management of cancer, since the majority of cancer mortality is associated with disseminated disease rather than the primary tumor. An essential requirement for the functionality of epithelial tissues is the maintenance of stable cell–cell contacts and cell polarity. This strict tissue organization is lost during the progression of epithelial tumors (carcinomas) and is particularly evident at the invasion stage (34). During the invasive process, tumor cells lose their cell–cell adhesion properties and frequently undergo profound changes in their

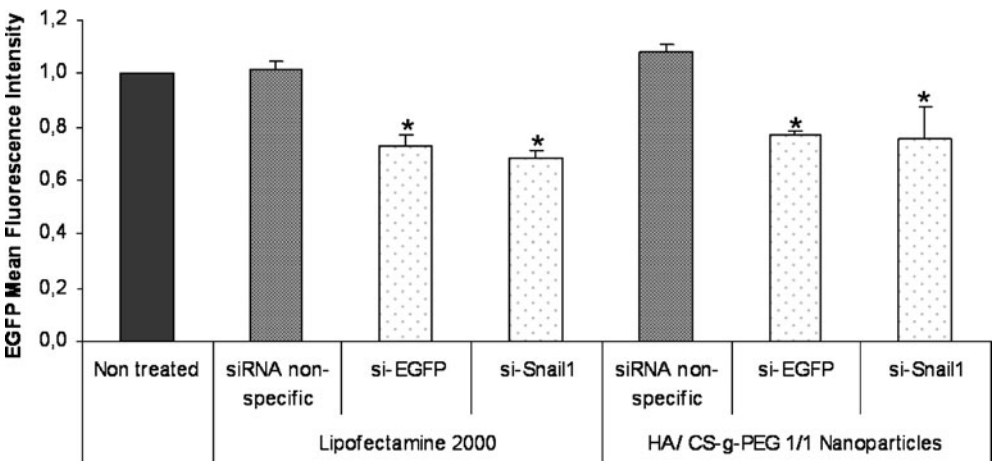

Fig. 10 Nanoparticle-mediated RNA interference in the HEK-EGFP-Snail1 cells. HA/CS-g-PEG 1/1 nanoparticles or Lipofectamine 2000 associating siRNA-Snail1 or siRNA-EGFP were incubated with the cells (100 nM siRNA/well). HA/CS-g-PEG 1/1 nanoparticles or Lipofectamine 2000 associating siRNA-non specific targeting controls are also shown. Results are expressed as mean±S.D. ($n=3$). Statistical differences are denoted as * ($p<0.05$).

phenotype, known as epithelial–mesenchymal transitions (EMTs) (35). This is due to the down-regulation of E-cadherin, a cell adhesion molecule that is critical for the maintenance of cell–cell contacts in epithelial tissues (36). In this context, the transcription factor Snail1 has been proposed as an important mediator of tumor invasion because of its role as a potent repressor of E-cadherin and strong inducer of EMT (14,37,38). Moreover, the Snail1 action has been recently corroborated through transient (39) or stable RNA interference (40,41) of the transcription factor in various cell systems. Overall, these observations have led to the identification of Snail1 as a potential therapeutic target to block tumor progression. To test the efficiency of siRNA nanoparticles to abrogate Snail1 expression, HEK293T cells stably expressing the fusion EGFP-Snail1 protein were generated (HEK-EGFP-Snail1 cells). In this cell line, EGFP-Snail1 knockdown can be either achieved with an effective delivery of si-EGFP or siRNA against the transcription factor Snail1 (si-Snail1), and in both cases effective knockdown will be reflected in a decrease in the EGFP mean fluorescence intensity. Therefore, HA/CS-g-PEG nanoparticles associating si-Snail1 were evaluated. HA/CS-g-PEG nanoparticles associating si-EGFP or a non-specific siRNA target were used as positive and negative controls, respectively. As can be seen in Fig. 10, HA/CS-g-PEG nanoparticles associating si-Snail1 significantly silenced EGFP-Snail1 expression compared to the non-treated cells. A similar level of EGFP-Snail1 knockdown was achieved with HA/CS-g-PEG nanoparticles associating siEGFP, thus corroborating the efficiency of the newly developed cell model and supporting the efficiency of the nanoparticles. HA/CS-g-PEG nanoparticles incorporating a non-specific target siRNA did not show any knockdown, evidence that the inhibition of the EGFP-Snail1 expression occurred through the sequence-specific RNAi effect. Moreover, no statistical difference could be observed between the gene knockdown ability of the HA/CS-g-PEG nanoparticles and the widely used commercial reagent Lipofectamine 2000. Additionally, HA/CS-g-PEG nanoparticles associating siRNA against Snail1 were evaluated in the HEK-EGFP cell line (Supplementary Material, Fig. 2), and no changes in the levels of EGFP expression could be detected. This result was expected, taking into consideration that no Snail1 expression could be detected the HEK-EGFP cell line as evaluated by western blot (Supplementary Material, Fig. 1). Moreover, the fact that the Snail1 transcription factor is not normally expressed in human cells and has always been identified in human carcinoma cell lines and tumours has already been reported by several authors [14]. For that reason, it is expected that the Snail1 transcription factor will not be affecting EGFP expression in HEK-EGFP cells.

In summary, these results suggest the potential application of HA/CS-g-PEG nanoparticles as a new anti-cancer therapeutic strategy.

CONCLUSION

Herein we report the development of a new versatile nanoparticle delivery system, consisting of HA and CS-g-PEG, which can be easily modulated and adapted for the delivery of different types of gene molecules, i.e. pDNA or siRNA. Irrespective of the greater ability of the nanoparticles to associate model pDNA compared to model siRNA, the results in cell culture experiments have shown their effectiveness in terms of facilitating (pDNA) or inhibiting (siRNA) gene expression. Moreover, these novel nanoparticles associating siRNA against the Snail1 transcription factor were able to efficiently inhibit its expression in the HEK-EGFP-Snail1 cell line. This interesting finding opens up new avenues for exploring novel cancer therapies based on the use and effective delivery of siRNA reagents.

ACKNOWLEDGEMENTS

The authors gratefully acknowledge valuable discussion with Dr. M. de la Fuente and support from the Ministry of Science and Technology (Spain) (Refs. SAF2004-09230-004-01 and SAF2004-C04-02). The first author also acknowledges the fellowship received from the Spanish Government (FPI).

REFERENCES

1. Elbashir SM, Harborth J, Lendeckel W, Yalcin A, Weber K, Tuschl T. Duplexes of 21-nucleotide RNAs mediate RNA interference in cultured mammalian cells. Nature. 2001;411:494–8.
2. Castanotto D, Rossi JJ. The promises and pitfalls of RNA-interference-based therapeutics. Nature. 2009;457:426–33.
3. MacLaughlin FC, Mumper RJ, Wang J, Tagliaferri JM, Gill I, Hinchcliffe M, *et al.* Chitosan and depolymerized chitosan oligomers as condensing carriers for *in vivo* plasmid delivery. J Control Release. 1998;56:259–72.
4. Gao S, Chen J, Dong L, Ding Z, Yang Y-h, Zhang J. Targeting delivery of oligonucleotide and plasmid DNA to hepatocyte via galactosylated chitosan vector. Eur J Pharm Biopharm. 2005;60:327–34.
5. Howard KA, Rahbek UL, Liu X, Damgaard CK, Glud SZ, Andersen MO, *et al.* RNA Interference *in vitro* and *in vivo* using a novel chitosan/siRNA nanoparticle system. Mol Ther. 2006;14:476–84.
6. Katas H, Alpar HO. Development and characterisation of chitosan nanoparticles for siRNA delivery. J Control Release. 2006;115:216–25.

7. de la Fuente M, Seijo B, Alonso MJ. Novel hyaluronan-based nanocarriers for transmucosal delivery of macromolecules. Macromol Biosci. 2008;8:441–50.
8. de la Fuente M, Seijo B, Alonso MJ. Bioadhesive hyaluronan-chitosan nanoparticles can transport genes across the ocular mucosa and transfect ocular tissue. Gene Ther. 2008;15:668–76.
9. de la Fuente M, Seijo B, Alonso MJ. Novel hyaluronic acid-chitosan nanoparticles for ocular gene therapy. Invest Ophthalmol Vis Sci. 2008;49:2016–24.
10. Csaba N, Koping-Hoggard M, Fernandez-Megia E, Novoa-Carballal R, Riguera R, Alonso MJ. Ionically crosslinked chitosan nanoparticles as gene delivery systems: effect of PEGylation degree on *in vitro* and *in vivo* gene transfer. J Biomed Nanotech. 2009;5:162–71.
11. Urban-Klein B, Werth S, Abuharbeid S, Czubayko F, Aigner A. RNAi-mediated gene-targeting through systemic application of polyethylenimine (PEI)-complexed siRNA *in vivo*. Gene Ther. 2005;12:461–6.
12. Minakuchi Y, Takeshita F, Kosaka N, Sasaki H, Yamamoto Y, Kouno M, et al. Atelocollagen-mediated synthetic small interfering RNA delivery for effective gene silencing *in vitro* and *in vivo*. Nucleic Acids Res 32: (2004).
13. Peinado H, Marin F, Cubillo E, Stark HJ, Fusenig N, Nieto MA, *et al.* Snail and E47 repressors of E-cadherin induce distinct invasive and angiogenic properties *in vivo*. J Cell Sci. 2004; 117:2827–39.
14. Cano A, Perez-Moreno MA, Rodrigo I, Locascio A, Blanco MJ, Del Barrio MG, *et al.* The transcription factor Snail controls epithelial-mesenchymal transitions by repressing E-cadherin expression. Nat Cell Biol. 2000;2:76–83.
15. Lamarque G, Lucas JM, Viton C, Domard A. Physicochemical behavior of homogeneous series of acetylated chitosans in aqueous solution: role of various structural parameters. Biomacromolecules. 2005;6:131–42.
16. Aktas Y, Yemisci M, Andrieux K, Gursoy RN, Alonso MJ, Fernandez-Megia E, *et al.* Development and brain delivery of chitosan-PEG nanoparticles functionalized with the monoclonal antibody OX26. Bioconj Chem. 2005;16:1503–11.
17. Prego C, Torres D, Fernandez-Megia E, Novoa-Carballal R, Quiñoa E, Alonso MJ. Chitosan-PEG nanocapsules as new carriers for oral peptide delivery: effect of chitosan pegylation degree. J Control Release. 2006;111:299–308.
18. Calvo P, Remuñan-Lopez C, Vila-Jato JL, Alonso MJ. Novel hydrophilic chitosan-polyethylene oxide nanoparticles as protein carriers. J Appl Polym Sci. 1997;63:125–32.
19. Peinado H, Ballestar E, Esteller M, Cano A. Snail mediates E-cadherin repression by the recruitment of the Sin3A/Histone deacetylase 1 (HDAC1)/HDAC2 complex. Mol Cell Biol. 2004;24:306–19.
20. Moreno-Bueno G, Peinado H, Molina P, Olmeda D, Cubillo E, Santos V, *et al.* The morphological and molecular features of the epithelial-to-mesenchymal transition. Nat Protoc. 2009;4:1591–613.
21. de la Fuente M, Seijo B, Alonso MJ. Design of novel polysaccharidic nanostructures for gene delivery. Nanotech. 2008;19:075105.
22. Bloomfield VA. DNA condensation. Curr Opin Struc Biol. 1996;6:334–41.
23. Bloomfield VA. DNA condensation by multivalent cations. Biopolymers. 1997;44:269–82.
24. Malek A, Czubayko F, Aigner A. PEG grafting of polyethylenimine (PEI) exerts different effects on DNA transfection and siRNA-induced gene targeting efficacy. J Drug Target. 2008;16:124–39.
25. Kabanov AV, Kabanov VA. DNA complexes with polycations for the delivery of genetic material into cells. Bioconj Chem. 1995;6:7–20.
26. Gary DJ, Puri N, Won YY. Polymer-based siRNA delivery: perspectives on the fundamental and phenomenological distinctions from polymer-based DNA delivery. J Control Release. 2007;121:64–73.
27. Bartlett DW, Davis ME. Physicochemical and biological characterization of targeted, nucleic acid-containing nanoparticles. Bioconj Chem. 2007;18:456–68.
28. Banan M, Puri N. The ins and outs of RNAi in mammalian cells. Curr Pharm Biotech. 2004;5:441–50.
29. Kabanov AV, Astafyeva IV, Chikindas ML, Rosenblat GF, Kiselev VI, Severin ES, *et al.* DNA interpolyelectrolyte complexes as a tool for efficient cell transformation. Biopolymers. 1991;31:1437–43.
30. Csaba N, Koping-Hoggard M, Alonso MJ. Ionically crosslinked chitosan/tripolyphosphate nanoparticles for oligonucleotide and plasmid DNA delivery. Int J Pharm. 2009;382:205–14.
31. Laurent TC, Fraser JRE. Hyaluronan. FASEB J. 1992;6:2397–404.
32. Rojanarata T, Opanasopit P, Techaarpornkul S, Ngawhirunpat T, Ruktanonchai U. Chitosan-thiamine pyrophosphate as a novel carrier for siRNA delivery. Pharm Res. 2008;25:2807–14.
33. Plattt VM, Szoka Jr FC. Anticancer therapeutics: targeting macromolecules and nanocarriers to hyaluronan or CD44, a hyaluronan receptor. Mol Pharm. 2008;5:474–86.
34. Stetler-Stevenson WG, Aznavoorian S, Liotta LA. Tumor cell interactions with the extracellular matrix during invasion and metastasis. Annu Rev Cell Biol. 1993;9:541–73.
35. Thiery JP. Epithelial–mesenchymal transitions in tumour progression. Nat Rev Cancer. 2002;2:442–54.
36. Birchmeier W, Behrens J. Cadherin expression in carcinomas: role in the formation of cell junctions and the prevention of invasiveness. Biochim Biophys Acta. 1994;1198:11–26.
37. Barrallo-Gimeno A, Nieto MA. The Snail genes as inducers of cell movement and survival: implications in development and cancer. Development. 2005;132:3151–61.
38. Peinado H, Olmeda D, Cano A. Snail, ZEB and bHLH factors in tumour progression: an alliance against the epithelial phenotype? Nat Rev Cancer. 2007;7:415–28.
39. Espineda CE, Chang JH, Twiss J, Rajasekaran SA, Rajasekaran AK. Repression of Na, K-ATPase β1-subunit by the transcription factor Snail in carcinoma. Mol Biol Cell. 2004;15:1364–73.
40. Olmeda D, Jorda M, Peinado H, Fabra A, Cano A. Snail silencing effectively suppresses tumour growth and invasiveness. Oncogene. 2007;26:1862–74.
41. Olmeda D, Moreno-Bueno G, Flores JM, Fabra A, Portillo F, Cano A. SNAI1 is required for tumor growth and lymph node metastasis of human breast carcinoma MDA-MB-231 cells. Cancer Res. 2007;67:11721–31.